MULTI FAULTS ESTIMATION IN ROTOR SYSTEMS USING CORRELATION ANALYSIS

Fabio Dalmazzo Sanches, fabiods@fem.unicamp.br
Robson Pederiva, robson@fem.unicamp.br
Faculty of Mechanical Engineering, State University of Campinas (Unicamp), Cidade Universitária "Zeferino Vaz", CEP: 13083-860, Campinas – SP, Brazil.

Abstract. *This work presents an identification methodology for multi-degree-of-freedom (mdofs) flexible rotor-bearing systems. The algorithm identifies two common faults occurring at the same time: the unbalance and the residual shaft bow, which contains magnitude and phase information, using only the rotor responses due to the combination of dynamic effects caused by the cited faults. As a way to overcome the practical difficulty with regard to the number of the available responses that can be measured, the proposed procedure uses the definition of coordinate transformation that is utilized in Lyapunov matrix equation. The system was modeled by state space representation and lumped-mass matrix. Through the definition of correlations used in matrix equation, it is possible to create an algorithm that correlates the system faults, consisted by magnitude and phase, to the correlation matrices of the measured state variables in time domain without the knowledge of the input forces. Numerical examples have been used to illustrate the developed algorithm considering also the effect of different noise levels in the rotor responses. The algorithm showed to be feasible and robust to be applied to real machines*.

Keywords: *Rotordynamics, Faults Identification, Correlation Analysis, Lyapunov Matrix Equation*

1. INTRODUCTION

The early detection of faults and malfunctions has been studied by many researchers due to its practical importance in industry which has machines with a high capital cost. So this is very important to avoid a more serious damage and huge financial losses. So the model-based diagnostic techniques are helpful tools to provide more significant fault information such as location and severity.

Unbalance, which is caused by the eccentricity of the mass from the geometric center, is one of the most common faults in rotating machines and it should be kept in a minimum level. The vibrations caused by it affect critical parts of the system such as bearings, seals, gears, motor, couplings etc.

One of typical reasons for an unbalance in a rotor is due to warping or static bending (permanent or temporary). These bowed rotors are encountered in practice for different reasons, e.g., letting a horizontal rotor rest for a long period of time or due to rubbing of a shaft on a seal (Rao, 2001). The bow and eccentricity are in general in different angular locations and bowed rotors behave somewhat different from purely unbalanced rotors (Rao, 2001 and Nicholas *et al.*, 1976).

This way, many contributions have been given to identify the unbalance, shaft bow and other kinds of faults and malfunctions, as multiple faults are common in real machines (Edwards *et al.*, 2000; Baschschmid *et al.*, 2002; Vania and Pennacchi., 2004). In general, the models have the same goal but they are different in mathematical approach and inclusion/representation of parts of the complete system: bearings, foundations, seals, etc. A general overview of model-based identification can be seen in Lees *et al.* (2009).

The methodology proposed in this paper uses the Lyapunov matrix equation and correlation analysis without the measuring of the input signals. The interest parameters are estimated from the correlations among the measured degrees of freedom. In rotor dynamics field, this method was used with white noise excitation and lumped mass matrix (Pederiva, 1992), unbalance plus stochastic input forces and artificial neural network to identify the fault parameters (Eduardo, 2003), random input and finite elements modeling to identify the bearing parameters (Sanches and Pederiva, 2009) and harmonic (unbalance) input in order to identify the fault parameters (Sanches and Pederiva, 2010).

This work is an extension of Sanches and Pederiva (2010) to the simultaneous identification of the unbalance and shaft bow parameters considering different fault configurations (magnitude and phase) and using only the rotor responses.

2. MATHEMATICAL MODELING

Considering that the rotor-bearing system, which is excited by harmonic forces due to unbalance and residual bow, can be modeled by a linear and time invariant mechanical system with n degrees of freedom, then the differential matrix equation that describes the physical system is (Rao, 2001):

$$[M]\{\ddot{\xi}(t)\}+[P]\{\dot{\xi}(t)\}+[K]\{\xi(t)\}=[H]\{n_1(t)\}+[B]\{n_2(t)\} \tag{1}$$

where $[M]$ is the mass matrix, $[P]$ is a matrix of speed proportional forces, $[K]$ is a matrix of displacements proportional forces, $\{\xi(t)\}$, $\{\dot{\xi}(t)\}$ and $\{\ddot{\xi}(t)\}$are the vectors corresponding to displacements, velocities and accelerations in this order, $[H]$ is the unbalance matrix, $[B]$ is the bow matrix.

The vectors $\{n_1(t)\}$ and $\{n_2(t)\}$ are the harmonic vectors referent to unbalance and shaft bow respectively. They are expressed as:

$$\{n_1(t)\} = \begin{Bmatrix} \sin(\Omega t + \beta) \\ \cos(\Omega t + \beta) \end{Bmatrix} \tag{2}$$

$$\{n_2(t)\} = \begin{Bmatrix} \sin(\Omega t + \alpha) \\ \cos(\Omega t + \alpha) \end{Bmatrix} \tag{3}$$

where Ω is the rotating frequency, β is the unbalance phase and α is the bow phase.

The matrices $[H]$ and $[B]$ can be given by:

$$[H] = \begin{bmatrix} 0 & 0 \\ \vdots & \vdots \\ m_u d\Omega^2 & 0 \\ 0 & m_u d\Omega^2 \\ 0 & 0 \\ \vdots & \vdots \\ 0 & 0 \end{bmatrix}_{(n,2)} \quad \text{and} \quad [B] = [K]\{\delta_r\} \tag{4}$$

m_u is the unbalance mass from the disks, d is the disk unbalance eccentricity with respect to the shaft geometric center and $\{\delta_r\}$ is the residual bow vector.

The rotor-bearing system described by Eq. (1) can also be expressed in state-space representation as:

$$\{\dot{x}(t)\} = [A]\{x(t)\} + [E_u]\{n_1(t)\} + [E_b]\{n_2(t)\} \tag{5}$$

where the state vector is given by:

$$\{x(t)\} = \begin{Bmatrix} \xi(t) \\ \cdots \\ \dot{\xi}(t) \end{Bmatrix} \tag{6}$$

and

$$[E_u] = \begin{bmatrix} 0 \\ \cdots \\ M^{-1}H \end{bmatrix}, \ [E_b] = \begin{bmatrix} 0 \\ \cdots \\ M^{-1}B \end{bmatrix} \tag{7}$$

The system output equation is:

$$\{y(t)\} = [C]\{x(t)\} \tag{8}$$

with [C] the output matrix.

The expression for the correlation matrix is defined by:

$$[R_{xx}(t,t+\tau)] = [R_{xx}(\tau)] = \varepsilon\{\{x(t)\}\{x^T(t+\tau)\}\} \tag{9}$$

where τ is a time delay instant and ε means the expected value between two terms.

Equations (2), (3) and (4) can be rewritten as (Lalanne and Ferraris, 1990):

$$[H] = \begin{bmatrix} 0 & 0 \\ \vdots & \vdots \\ a\Omega^2 & b\Omega^2 \\ -b\Omega^2 & a\Omega^2 \\ 0 & 0 \\ \vdots & \vdots \\ 0 & 0 \end{bmatrix}_{(n,2)} \quad \text{and} \quad [B] = \begin{bmatrix} 0 & 0 \\ \vdots & \vdots \\ c & d \\ -d & c \\ 0 & 0 \\ \vdots & \vdots \\ 0 & 0 \end{bmatrix}_{(n,2)} \tag{10}$$

and

$$\{n_1(t)\} = \{n_2(t)\} = \{n(t)\} = \begin{Bmatrix} \sin(\Omega t) \\ \cos(\Omega t) \end{Bmatrix} \tag{11}$$

with

$$a = m_u d \cos\beta \ \text{ and } \ b = m_u d \sin\beta \tag{12}$$

$$c = k_{i,j}\delta_{r_s} \cos\alpha \ \text{ and } \ d = k_{i,j}\delta_{r_s} \sin\alpha \tag{13}$$

where $k_{i,j}$ are terms from the stiffness matrix and δ_{rs} represents the residual bow at some shaft position.

Applying Eq. (9) to Eq. (5) and using Eqs. (10) to (13), it is possible to obtain an equation that correlates the system outputs with the rotor fault parameters and the physical system parameters (Pederiva, 1992 and Eduardo, 2003). This equation is called *Generalized Lyapunov Matrix Equation* for systems excited by harmonic forces:

$$[A][R_{xx}(\tau_i)] + [R_{xx}(\tau_i)][A]^T + [E][R_{nx}(\tau_i)] + [R_{xn}(\tau_i)][E]^T = 0 \tag{14}$$

with

$$[E] = [E_u] + [E_b] \tag{15}$$

$$[A] = \begin{bmatrix} 0_{(n,n)} & I_{(n,n)} \\ -M^{-1}K & -M^{-1}P \end{bmatrix} = \begin{bmatrix} 0_{(n,n)} & I_{(n,n)} \\ A_1 & A_2 \end{bmatrix} \tag{16}$$

and

$$[P] = [D] + \Omega[G] \tag{17}$$

where [D] is the damping matrix and [G] is the gyroscopic matrix.

Considering that the rotor system is excited only by harmonic forces, in this studied case caused by unbalance and shaft bow combined, the state vector assumes the following form:

$$\{x(t)\} = z_1 \sin(\Omega t) + z_2 \cos(\Omega t) \tag{18}$$

where z_1 and z_2 are general numbers.

2.1. Reduction of the system measured outputs

All the assumptions considered previously took into consideration that the entire state vector is measured. In practice this does not occur because some degrees of freedom are not available by reasons that include safety and difficulties to access some measuring points on the machine. This way, an output measurement reduction should be considered in order to work with a more realistic situation that enables this methodology to be applied in real rotating machines.

It is known that velocity and displacement measurements are redundant considering the system observability and this represents a natural output reduction. So, with only the displacements it is possible to observe completely the system (Pederiva, 1992). The goal is not only to exclude the velocities but also to provide an addition reduction with respect to the number of displacements acquired by transducers.

Considering that the entire state vector is not available, Eq. (14) cannot be applied and additional correlations should be used to replace the missing ones.

In order to replace the missing state variables and to generate additional data to be used in the identification process, Pederiva (1992) proposes the utilization of a filter system. Figure 1 shows how the filter acts in the mechanical system.

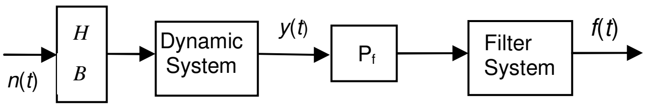

Figure 1. Schematic representation of the dynamic system + filter

The filter system is represented by the state-space equation:

$$\left[\dot{f}(t)\right] = [N]\{f(t)\} + \left[P_f\right]\{y(t)\} \tag{19}$$

with:

$$\left\{f^T(t)\right\} = \left\{\eta_1 \quad \eta_2 \quad \cdots \quad \eta_q\right\}_{(1,q)} \tag{20}$$

η_1 to η_q are the filter outputs.

The filter matrix is:

$$[N] = \begin{bmatrix} 0 & 1 & 0 & 0 & \cdots & 0 \\ 0 & 0 & 1 & 0 & \cdots & 0 \\ \vdots & \vdots & \vdots & \vdots & \ddots & \vdots \\ 0 & 0 & 0 & 0 & \cdots & 1 \\ n_1 & n_2 & n_3 & n_4 & \cdots & n_q \end{bmatrix}_{(q,q)} \tag{21}$$

and the input filter matrix:

$$[P_f]=\begin{bmatrix}0 & 0 & \cdots & 0\\ \vdots & \vdots & \ddots & \vdots\\ 0 & 0 & 0 & 0\\ p_1 & p_2 & \cdots & p_m\end{bmatrix}_{(q,m)} \tag{22}$$

The filter system has order q and it is stable and controllable. The parameters n_1 to n_q are filter parameters, p_1 to p_m are the input filter parameters and the index m is the number of available measured outputs.

When a reduction of the measured state variables is performed, the system must continue to be observable by the available variables that are possible to be acquired. Dynamic systems described as showed by Eqs. (5) and (8) can be represented in many different ways which are known as normal forms of state equation and these new forms have other coordinate systems, so the input/output system description changes as well as the input/output system matrices.

Through a specific coordinate base, it is possible to obtain transformed matrices $[A^*]$, $[B^*]$ and $[C^*]$ that contain simple internal structures which can be easily used in a parameter estimation algorithm. These special structures are obtained by the choice of specific coordinate transformation basis.

This way, changing the coordinate basis:

$$\{x^*(t)\}=[T]\{x(t)\} \tag{23}$$

where $[T]$ is the coordinate transformation matrix.

Performing a coordinate transformation in the studied system:

$$\{\dot{x}^*\}=[A^*]\{x^*(t)\}+[E^*]\{n(t)\} \tag{24}$$

Considering the original rotating system completely observable, it is desirable that this condition be still valid with a reduction of the output measurements. In other words, the transformation matrix should be conveniently chosen. To guarantee the system observability in the case of having some parts of the state vector, the transformation matrix used to rewrite the rotating system will be the observability matrix.

Applying this kind of coordinate transformation to the rotor system, the matrices $[A^*]$ and $[C^*]$ have special structures (Pederiva, 1992) that are very useful to have an identification algorithm.

As mentioned previously a filter system is used to generate additional data to replace the missing correlations. This way the complete system is formed by the rotating system plus the filter and this *expanded system* is described by:

$$\{\dot{x}_e(t)\}=[A_e^{'}]\{x_e(t)\}+[E_e^{'}]\{n(t)\} \tag{25}$$

with

$$\{x_e(t)\}=\begin{Bmatrix}x^*(t)\\ f(t)\end{Bmatrix} \tag{26}$$

$$[A_e^{'}]=\begin{bmatrix}A^* & 0\\ P_f C^* & N\end{bmatrix} \tag{27}$$

and

$$[E_e^{'}]=\begin{bmatrix}E^*\\ 0\end{bmatrix} \tag{28}$$

The Lyapunov matrix equation described by Eq. (14) can be represented in a general form to the expanded system as:

$$[A'][R'] + [R'][A']^T = [Q'] \tag{29}$$

2. ROTOR SIMULATIONS

The system to be considered is composed by a flexible shaft supported on two identical rolling bearings with two independent unbalanced disks and the shaft bow is presented at the disks position. A general view of the rotating system is showed by the Fig.2.

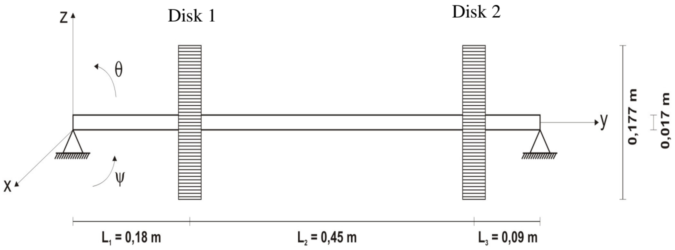

Figure 2. Representation of the rotating system

The system described by Fig. 2 was modeled by lumped mass matrix and this kind of modeling applied to rotors is described by Gasch and Knothe (1987). In this modeling, all the rotor mass comes from the disks which are heavier than the shaft. This approach is simpler than modeling by finite elements and provides a good first identification of the fault parameters.

Details of the coordinate system used to model the rotor as well as the mass and gyroscopic matrix can be seen in Lalanne and Ferraris (1990). The damping matrix is diagonal and the system has 8 degrees of freedom, 4 linear coordinates and 4 angular ones.

Considering that the angular displacements are difficult to be acquired by transducers, the simulations take in consideration only the linear measurements at disks position (1/4 of the state vector) which is closer to a real situation.

Taking into account these assumptions, the transformations matrix for this studied case is given by:

$$[T]^T = [C \quad C.A \quad C.A^2 \quad C.A^3] \tag{30}$$

To identify the system, it is proposed a filter of order 6 (Sanches and Pederiva, 2009) that will be used in Eq. (29) which will generate the identification algorithms through its matrices $[A^{'}]$ and $[R^{'}]$. Details of these two matrices can be seen in Sanches and Pederiva (2010). The matrix $[Q^{'}]$ contains the fault parameters and it has the following structure:

$$[Q'] = \begin{bmatrix} 0_{(4,4)} & \vdots & & \vdots & 0_{(4,6)} \\ \cdots & \vdots & Q_{1_{(16,12)}} & \vdots & \cdots \\ Q_{2_{(12,4)}} & \vdots & & \vdots & Q_{4_{(12,6)}} \\ \cdots & \cdots & \cdots & \cdots & \cdots \\ 0_{(6,4)} & \vdots & Q_{3_{(6,12)}} & \vdots & 0_{(6,6)} \end{bmatrix} \tag{31}$$

where Q_1, Q_2, Q_3 and Q_4 are sub matrices of $[Q^{'}]$.

Equation (31) comes from Eq.(14) for the expanded system and it is given by:

$$[Q'] = -\left([E_e'][R_{nx_e}](\tau_i) + [R_{x_e n}(\tau_i)][E_e']^T\right) \tag{32}$$

The unbalance parameters for each disk as well as a general view of the shaft bow are showed by Fig. 3:

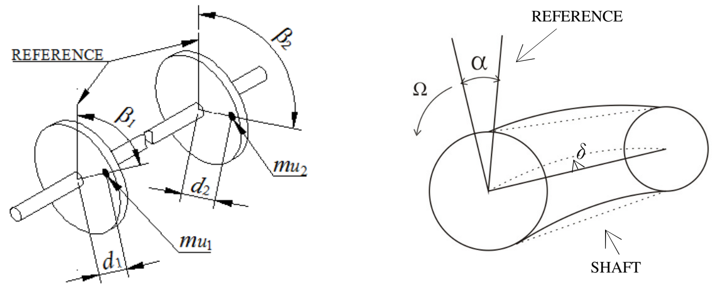

Figure 3. Representation of unbalance and shaft bow

To simulate the system, the bow was considered at the disks position. This way the shaft bow parameters are:

$$c_1 = \left(k_{1,1}\delta_{r_1} + k_{1,5}\delta_{r_2}\right)\cos\alpha_1 \quad \text{and} \quad d_1 = \left(k_{2,2}\delta_{r_1} + k_{2,6}\delta_{r_2}\right)\sin\alpha_1 \tag{33}$$

$$c_2 = \left(k_{5,1}\delta_{r_1} + k_{5,5}\delta_{r_2}\right)\cos\alpha_2 \quad \text{and} \quad d_2 = \left(k_{6,2}\delta_{r_1} + k_{6,6}\delta_{r_2}\right)\sin\alpha_2 \tag{34}$$

where the subscripts 1 and 2 are referent to the shaft bow present at disks 1 and 2 position, respectively. The variable δ represents the residual bending presented by the shaft due to, for example, its weight, bad mounting or inaccuracies on the machining process.

The sub matrices Q_1, Q_2, Q_3 and Q_4 from Eq. (31) are given in function of the unbalance parameters (a and b), the shaft bow parameters (c and d), and the coefficients z given by Eq. (18) whose calculations are given in details by Sanches and Pederiva (2010). Sub matrix Q_3 is the only one that will be used in the identification algorithm and it comes from the correlations between the filter outputs $\{f(t)\}$ and the harmonic vector $\{n(t)\}$.

Working with specific rows and columns in the matrices given by Eq. (29), it is possible to obtain the estimation equation that involves the fault parameters and the correlation matrices between the filter outputs and the measured state variables (Sanches and Pederiva, 2010):

$$S_5 - S_3 - r_{\eta_5 x_m^*} + \left[r_{\eta_1 x_m^*} \;\vdots\; r_{\eta_2 x_m^*} \;\vdots\; S_1 + r_{\eta_3 x_m^*} \;\vdots\; S_4 - S_2 - r_{\eta_4 x_m^*} \right] [\theta]^* = S_8 \tag{35}$$

The terms S are corresponding parts of the sub matrix Q_3 showed by Eq. (31), $r_{\eta_i x_m^*}$ is the correlation between the ith filter output and the measured displacements, and:

$$[\theta]^* = \begin{bmatrix} A_1^{*T} \\ A_2^{*T} \end{bmatrix}_{(16,4)} \tag{36}$$

2.1. Numerical results

The filter parameters in Eqs. (21) and (22) were chosen based on the system stability and these values were described in details in Sanches and Pederiva (2009).

The rotor damping matrix was chosen in such a way that the damping factor is 4.3% to simulate a more realistic situation. This way, the first two natural frequencies of the rotating system are 31 Hz and 88 Hz and the first filter frequency is 228 Hz, so none rotor response will be smoothed until the second critical frequency (Sanches and Pederiva, 2010). These frequencies are showed by Fig. (4).

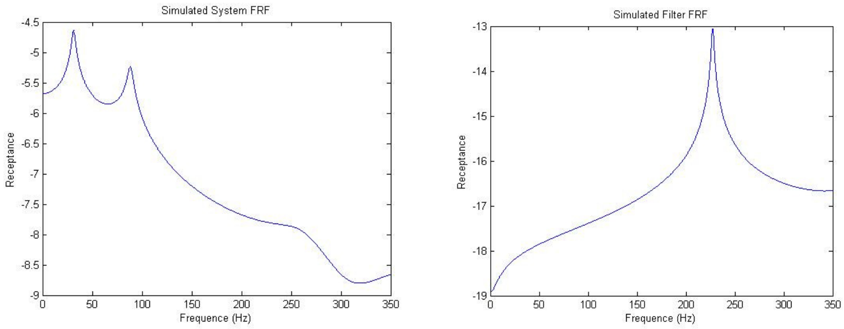

Figure 4. System and filter FRFs

To estimate the fault parameters, it was used in Eq. (35) three time delays τ_i and three different rotating speeds. Simulations were performed considering four different situations for two theoretical fault configurations given by Tab. 1. In order to have more tests on the robustness of this method, configuration 2 was simulated with random noise of 2% and 4% in the system outputs. To estimate all the fault parameters, it was used the least square method applied to Eq. (35).

Table 1. Two simulated fault configurations

Configuration 1	Configuration 2
$m_{u1}d_1 = 1{,}5.10^{-4}$ Kg.m, $m_{u2}d_2 = 3{,}16.10^{-4}$ Kg.m	$m_{u1}d_1 = 3.10^{-4}$ Kg.m, $m_{u2}d_2 = 1{,}58.10^{-4}$ Kg.m
$\beta_1 = 200^0$, $\beta_2 = 320^0$	$\beta_1 = 70^0$, $\beta_2 = 130^0$
$\delta_{r1} = 20.10^{-6}$ m, $\delta_{r2} = 12.10^{-6}$ m	$\delta_{r1} = 10.10^{-6}$ m, $\delta_{r2} = 25.10^{-6}$ m
$a_1 = 190^0$, $a_2 = 350^0$	$a_1 = 160^0$, $a_2 = 250^0$

The following tables show the simulation results for the unbalance and shaft bow parameters identification considering various situations described in the further cases. In these simulations it was not considered the noise effect on the system outputs.

<u>Case 1</u>: Simulations considering three rotating frequencies below the first critical speed: 20, 25 and 30Hz. The results are showed by Tab. 2:

Tab 2. Simulation results under the first critical speed

Config.1	Error	Config.1	Error	Config.2	Error	Config.2	Error
$m_{u1}d_1 = 1{,}5116.10^{-4}$	0,77%	$\delta_{r1} = 19{,}96.10^{-6}$	0,20%	$m_{u1}d_1 = 2{,}99.10^{-4}$	0,03%	$\delta_{r1} = 9{,}89.10^{-6}$	1,10%
$\beta_1 = 200{,}45^0$	0,23%	$a_1 = 189{,}85^0$	0,08%	$\beta_1 = 70{,}733^0$	1,05%	$a_1 = 159{,}57^0$	0,27%
$m_{u2}d_2 = 3{,}15.10^{-4}$	0,32%	$\delta_{r2} = 12.10^{-6}$	0,00%	$m_{u2}d_2 = 1{,}594.10^{-4}$	0,89%	$\delta_{r2} = 24{,}99.10^{-6}$	0,04%
$\beta_2 = 319{,}81^0$	0,06%	$a_2 = 350{,}01^0$	0,01%	$\beta_2 = 130{,}57^0$	0,44%	$a_2 = 250{,}02^0$	0,01%

<u>Case 2</u>: Simulations considering three rotating frequencies above the first critical speed: 45, 60 and 75Hz. The results are showed by Tab. 3:

Tab 3. Simulation results above the first critical speed

Config.1	Error	Config.1	Error	Config.2	Error	Config.2	Error
$m_{u1}d_1 = 1{,}51.10^{-4}$	0,67%	$\delta_{r1} = 19{,}78.10^{-6}$	1,10%	$m_{u1}d_1 = 3{,}00.10^{-4}$	0,00%	$\delta_{r1} = 10{,}17.10^{-6}$	1,70%
$\beta_1 = 198{,}78^0$	0,61%	$a_1 = 191{,}05^0$	0,55%	$\beta_1 = 69{,}67^0$	0,47%	$a_1 = 158{,}78^0$	0,76%
$m_{u2}d_2 = 3{,}224.10^{-4}$	2,03%	$\delta_{r2} = 11{,}86.10^{-6}$	1,17%	$m_{u2}d_2 = 1{,}573.10^{-4}$	0,44%	$\delta_{r2} = 25.10^{-6}$	0,00%
$\beta_2 = 320{,}24$	0,08%	$a_2 = 350{,}27^0$	0,08%	$\beta_2 = 132{,}38^0$	1,83%	$a_2 = 250{,}15^0$	0,06%

The simulation results from cases 1 and 2 are considered good especially when the estimation is performed using rotating speeds under the first critical speed. In case 2, the estimations are still good and the algorithm seems to be robust considering different rotating frequencies.

In the following two cases, simulations will be performed mixing frequencies under and above the first critical speed. The goal here is to investigate if the phase inversion that occurs after passing through the first critical speed will disturb the estimation results.

<u>Case 3</u>: Simulations considering two rotating frequencies under the first critical speed (25 and 30Hz) and one frequency above it: 45Hz. The results are showed by Tab. 4 and noise was not considered.

Tab 4. Simulation results considering a mix of rotating frequencies

Config.1	Error	Config.1	Error	Config.2	Error	Config.2	Error
$m_{u1}d_1 = 1,4978.10^{-4}$	0,15%	$\delta_{r1} = 20,03.10^{-6}$	0,15%	$m_{u1}d_1 = 3,001.10^{-4}$	0,03%	$\delta_{r1} = 10,04.10^{-6}$	0,40%
$\beta_1 = 199,31^0$	0,35%	$a_1 = 190,49^0$	0,26%	$\beta_1 = 70,253^0$	0,36%	$a_1 = 160,43^0$	0,27%
$m_{u2}d_2 = 3,1625.10^{-4}$	0,08%	$\delta_{r2} = 11,99.10^{-6}$	0,08%	$m_{u2}d_2 = 1,585.10^{-4}$	0,32%	$\delta_{r2} = 24,87.10^{-6}$	0,52%
$\beta_2 = 320,14$	0,04%	$a_2 = 349,95^0$	0,01%	$\beta_2 = 130,33^0$	0,25%	$a_2 = 249,99^0$	0,01%

Case 4: Simulations considering two rotating frequencies above the first critical speed (45 and 60Hz) and one frequency under it: 30Hz. The results are showed by Tab. 5 and noise was not considered.

Tab 5. Simulation results considering a mix of rotating frequencies

Config.1	Error	Config.1	Error	Config.2	Error	Config.2	Error
$m_{u1}d_1 = 1,4978.10^{-4}$	0,15%	$\delta_{r1} = 20,03.10^{-6}$	0,15%	$m_{u1}d_1 = 3,008.10^{-4}$	0,27%	$\delta_{r1} = 10,26.10^{-6}$	2,60%
$\beta_1 = 199,23^0$	0,39%	$a_1 = 190,57^0$	0,30%	$\beta_1 = 69,654^0$	0,49%	$a_1 = 160,87^0$	0,54%
$m_{u2}d_2 = 3,172.10^{-4}$	0,38%	$\delta_{r2} = 11,98.10^{-6}$	0,17%	$m_{u2}d_2 = 1,571.10^{-4}$	0,57%	$\delta_{r2} = 25.10^{-6}$	0,00%
$\beta_2 = 320,17$	0,05%	$a_2 = 349,96^0$	0,01%	$\beta_2 = 130,47^0$	0,36%	$a_2 = 249,97^0$	0,01%

The tables from the two previous cases show that mixing frequencies below and after the first critical one, the estimations continue to be precise and there is no influence of the phase inversion on the obtained results.

In the next simulated cases, configuration 2 will be tested in the presence of random noise on the rotor outputs. It is known that noise is very common in experimental test rigs and they cause some distortions on the estimations and it is very important to test the robustness of the applied methodology in the presence of this kind of problem since the system outputs are the filter ones and the uncontrolled filter outputs are subjected to the input noise.

Case 5: Simulations with random noise of 2% and 4% considering three rotating frequencies below the first critical speed: 20, 25 and 30Hz. The results are showed by Tab. 6:

Tab 6. Simulation results under the first critical speed considering noise

Noise: 2%	Error	Noise: 2%	Error	Noise: 4%	Error	Noise: 4%	Error
$m_{u1}d_1 = 2,985.10^{-4}$	0,77%	$\delta_{r1} = 9,57.10^{-6}$	4,30%	$m_{u1}d_1 = 3,062.10^{-4}$	2,07%	$\delta_{r1} = 9,09.10^{-6}$	9,10%
$\beta_1 = 72,866^0$	4,09%	$a_1 = 160,36^0$	0,22%	$\beta_1 = 76,577^0$	9,40%	$a_1 = 164,58^0$	2,86%
$m_{u2}d_2 = 1,613.10^{-4}$	2,09%	$\delta_{r2} = 24,99.10^{-6}$	0,00%	$m_{u2}d_2 = 1,709.10^{-4}$	8,16%	$\delta_{r2} = 25.10^{-6}$	0,00%
$\beta_2 = 130,52^0$	0,40%	$a_2 = 250,03^0$	0,01%	$\beta_2 = 130,83^0$	0,64%	$a_2 = 250,09^0$	0,04%

Case 6: Simulations considering random noise and three rotating frequencies above the first critical speed: 45, 60 and 75Hz. The results are showed by Tab. 7:

Tab 7. Simulation results above the first critical speed considering noise

Noise: 2%	Error	Noise: 2%	Error	Noise: 4%	Error	Noise: 4%	Error
$m_{u1}d_1 = 3,007.10^{-4}$	0,23%	$\delta_{r1} = 10,15.10^{-6}$	1,50%	$m_{u1}d_1 = 3,019.10^{-4}$	0,63%	$\delta_{r1} = 9,93.10^{-6}$	0,70%
$\beta_1 = 69,726^0$	0,39%	$a_1 = 161,41^0$	0,88%	$\beta_1 = 69,939^0$	0,09%	$a_1 = 165,87^0$	3,67%
$m_{u2}d_2 = 1,579.10^{-4}$	0,06%	$\delta_{r2} = 24,86.10^{-6}$	0,56%	$m_{u2}d_2 = 1,596.10^{-4}$	1,01%	$\delta_{r2} = 24,86.10^{-6}$	0,56%
$\beta_2 = 132,06^0$	1,58%	$a_2 = 250,20^0$	0,08%	$\beta_2 = 131,55^0$	1,19%	$a_2 = 250,31^0$	0,12%

Case 7: Simulations considering random noise, two rotating frequencies under the first critical speed (25 and 30Hz) and one frequency above it: 45Hz. The results are showed by Tab. 8.

Tab 8. Simulation results considering a mix of rotating frequencies and input noise

Noise: 2%	Error	Noise: 2%	Error	Noise: 4%	Error	Noise: 4%	Error
$m_{u1}d_1 = 3,003.10^{-4}$	0,10%	$\delta_{r1} = 10,05.10^{-6}$	0,50%	$m_{u1}d_1 = 3,035.10^{-4}$	1,17%	$\delta_{r1} = 10,29.10^{-6}$	2,90%
$\beta_1 = 71,275^0$	1,82%	$a_1 = 161,57^0$	0,98%	$\beta_1 = 72,691^0$	3,84%	$a_1 = 163,02^0$	1,89%
$m_{u2}d_2 = 1,588.10^{-4}$	0,51%	$\delta_{r2} = 25,01.10^{-6}$	0,04%	$m_{u2}d_2 = 1,617.10^{-4}$	2,34%	$\delta_{r2} = 25,04.10^{-6}$	0,16%
$\beta_2 = 129,72^0$	0,22%	$a_2 = 249,96^0$	0,02%	$\beta_2 = 129,02^0$	0,75%	$a_2 = 249,87^0$	0,05%

Case 8: Simulations considering random noise, two rotating frequencies above the first critical speed (45 and 60Hz) and one frequency under it: 30Hz. The results are showed by Tab. 9.

Tab 9. Simulation results considering a mix of rotating frequencies and input noise

Noise: 2%	Error	Noise: 2%	Error	Noise: 4%	Error	Noise: 4%	Error
$m_{u1}d_1 = 3,01.10^{-4}$	0,33%	$\delta_{r1} = 10,81.10^{-6}$	8,10%	$m_{u1}d_1 = 3,00.10^{-4}$	0,00%	$\delta_{r1} = 11,96.10^{-6}$	19,6%
$\beta_1 = 69,22^0$	1,11%	$a_1 = 161,88^0$	1,18%	$\beta_1 = 68,279^0$	2,46%	$a_1 = 160,29^0$	0,18%
$m_{u2}d_2 = 1,574.10^{-4}$	0,38%	$\delta_{r2} = 25,03.10^{-6}$	0,12%	$m_{u2}d_2 = 1,561.10^{-4}$	1,20%	$\delta_{r2} = 25,06.10^{-6}$	0,24%
$\beta_2 = 129,89^0$	0,08%	$a_2 = 249,93^0$	0,03%	$\beta_2 = 129^0$	0,77%	$a_2 = 249,74^0$	0,11%

The simulated cases considering the noise effect presented satisfactory results and some fault parameters were identified with the same accuracy of the cases in which noise was not considered. Probably one way to improve the identification processes is using more rotating frequencies in order to take in account more dynamic effects of the rotating system.

3. CONCLUSIONS

An identification method for unbalance and shaft bow parameters estimation was presented for *mdof* rotor-bearing system. This simpler modeling (Gasch and Knothe, 1987), in which the bearing parameters are not considered, provides an easier fault parameters identification and provides a good first approach to model rotating systems. This proposed method is based on Lyapunov matrix equation and the correlation matrices involving the measured outputs and the filter ones.

One way to improve this methodology is to reduce the number of delay instants and to improve the number of rotating frequencies after and below the first critical speed, this way more dynamic effects will be taken in account in the identification process.

Special attention should be given to filter system in such a way that any important information does not be smoothed in the range of interest and additional information be generated to become possible the faults identification.

The estimation results are considered satisfactory and the estimator identifies the fault parameters with accuracy and robustness even in the presence of noise and considering the combined unbalance and shaft effects. The next step of this work is to validate the described algorithm using experimental data from a test rig, which is presented in the Laboratory of Vibrations and Control located in Unicamp.

4. REFERENCES

Bachschmid, N., Pennacchi, P. and Vania, A., 2002, "Identification of Multiple Faults in Rotor Systems". Journal of Sound and Vibration, Vol. 254, No. 2, pp. 327-366.

Eduardo, A.C., 2003, "Fault Diagnosis in Rotor Systems through Correlation Analysis and Artificial Neural Networks". Ph.D. Thesis, Faculty of Mechanical Engineer, University of Campinas, BR. In Portuguese.

Edwards, S., Lees, A.W. and Friswell, M.I., 2000, "Experimental Identification of Excitation and Support Parameters of a Flexible Rotor-Bearing-Foundation System from a Single Run-Down". Journal of Sound and Vibration, Vol. 232, No. 5, pp. 963-992.

Gasch, R. and Knothe, K., 1987, "Strukturdynamik: Diskrete Systeme: band 1", Ed. Springer-Verlag, Berlin, Germany, pp. 101-105.

Lalanne, M. and Ferraris, G., 1990, "Rotordynamics Prediction in Engineering", Ed. John Wiley and Sons, West Sussex, 198 p.

Lees, A.W., Sinha, J.K. and Friswell, M.I., 2009, "Model-Based Identification of Rotating Machines". Mechanical Systems and Signal Processing, Vol. 23, pp. 1884-1893.

Nicholas, J.C., Gunter, E.J. and Allaire, P.E., 1976, "Effect of Residual Shaft Bow on Unbalance Response and Balancing of a Single Mass Flexible Rotor – Part 1: Unbalance Response". Journal of Engineering for Power, Vol. 98, No. 2, pp. 171-181.

Pederiva, R., 1992, "Parametric Identification of Stochastically Excited Mechanical Systems". Ph.D. Thesis, Faculty of Mechanical Engineer, University of Campinas, BR. In Portuguese.

Rao, J.S., 2001, "A Note on Jeffcott Warped Rotor". Mechanism and Machine Theory, Vol. 36, pp. 563-575.

Sanches, F.D. and Pederiva, R., 2009, "Bearing Parameters Estimation using Correlation Analysis and Random Response", Proceedings of the 20th International Congress of Mechanical Engineering, Gramado, Brazil.

Sanches, F.D. and Pederiva, R., 2010, "Identification of the Unbalance using Correlation Analysis and Unbalance Responses", Proceedings of the 8th IFToMM International Conference on Rotordynamics, Seoul, Korea.

Vania, A. and Pennacchi, P., 2004, "Experimental and Theoretical Application of Fault Identification Measures of Accuracy in Rotating Machine Diagnostics". Mechanical Systems and Signal Processing, Vol. 18, pp. 329-352.

5. RESPONSIBILITY NOTICE